PROCEEDINGS OF SCIENCE

Hunting for leptoquarks

Felix Wilsch*

Institute for Theoretical Particle Physics and Cosmology, RWTH Aachen University, Sommerfeldstr. 16, D-52054 Aachen, Germany

E-mail: felix.wilsch@physik.rwth-aachen.de

Leptoquark (LQ) models have received increased interest in recent year as compelling explanations of the charged-current B-meson anomalies known as $R_{D^{(*)}}$ and the resulting indication of lepton-flavor non-universality. At the LHC, leptoquarks can be searched for in various channels, including pair, single, and resonant production, as well as Drell-Yan. We summarize these different channels and their complementarity. Furthermore, we review the current status of the leptoquark models that can address the $R_{D^{(*)}}$ anomalies. To that end, we consider the most recent data sets from high-p_T tails at the LHC and low-energy precision measurements and highlight their complementary. Moreover, we comment on the future perspectives for LHC searches for these models.

12th Large Hadron Collider Physics Conference (LHCP2024)
3-7 June 2024
Boston, USA

*Speaker

PoS(LHCP2024)006

1. Introduction

Leptoquarks are hypothetical particles that are introduced in many BSM theories, such as Pati-Salam models, GUTs, or technicolor. LQs unify matter by carrying both Baryon and lepton number. Thus, semi-leptonic transitions offer a unique possibility to probe these exotic states. A list of all LQs and their interactions with the SM fermions has been compiled in [1, 2]. In recent years, there has been an increased interest in LQ models as they can be used to address the charged current B-meson anomalies. For the latest status update, see [3]. If confirmed, these anomalies would indicated lepton-flavor non-universality and possibly new physics contributing to the $b \to c\tau\nu$ transitions. Therefore, models with dominant LQs couplings to third generation SM fermions are particularly relevant in light of these anomalies. Only three LQs are in principle capable of explaining the $R_{D^{(*)}}$ anomalies [4], namely one vector LQ dubbed $U_1 \sim (\mathbf{3}, \mathbf{1})_{2/3}$ and two scalar LQs named $S_1 \sim (\bar{\mathbf{3}}, \mathbf{1})_{1/3}$ and $R_2 \sim (\mathbf{3}, \mathbf{2})_{7/6}$. Their interaction Lagrangians are given by

$$\mathcal{L}^{\text{int}}_{U_1} = [x_1^L]_{i\alpha}\bar{q}_i \not{U}_1 \ell_\alpha + [x_1^R]_{i\alpha}\bar{d}_i \not{U}_1 e_\alpha + \text{H.c.}\,, \tag{1a}$$

$$\mathcal{L}^{\text{int}}_{S_1} = [y_1^L]_{i\alpha} S_1 \bar{q}_i^c \varepsilon \ell_\alpha + [y_1^R]_{i\alpha} S_1 \bar{u}_i^c e_\alpha + \text{H.c.}\,, \tag{1b}$$

$$\mathcal{L}^{\text{int}}_{R_2} = [y_2^L]_{i\alpha}\bar{u}_i \ell_\alpha \varepsilon R_2 + [y_2^R]_{i\alpha}\bar{q}_i e_\alpha R_2 + \text{H.c.}\,. \tag{1c}$$

In the following, we will review the different channels that are employed for LQ searches at the LHC in Sec. 2. Thereafter, in Sec. 3 we will analyze the three LQ models mentioned above in light of the B-anomalies, paying special attention to the complementarity of high- and low-energy data.

2. Experimental studies

Due to the nature of LQs, flavor experiments provide an ideal laboratory to constrain the flavor patterns of their couplings with precision measurements of semi-leptonic transitions. These low-energy analyses are usually performed in an Effective Field Theory (EFT) setup, see e.g. [5, 6]. Subsequently, the EFT coefficients can be related to the couplings and masses of the LQ models by matching calculations. With the LHC run-II, also the high-p_T data sets collected by the ATLAS and CMS experiments became competitive for studying LQ models. At these higher energies, analyses are often performed in the full model rather than in the corresponding EFT due to questions regarding the validity of the EFT approach. However, EFT analyses of LQ models are also possible at high-p_T, see e.g. [7]. In the following, we will focus on direct searches for LQ models.

2.1 High-p_T searches for leptoquarks at the LHC

LQs can be produced in different ways at the LHC, leading to various experimental signatures. The most important channels for LQ searches at the LHC are shown in Fig. 2 and include: (a) LQ pair production, which is QCD initiated and proportional to the strong coupling; (b) single production of a resonant LQ in quark-gluon fusion; (c) non-resonant Drell-Yan production, where the LQ is mediated in the t- or u-channel; and (d) resonant s-channel LQ production in quark-lepton fusion processes, which are initiated by the small lepton contribution to the proton PDFs [8]. In the following, we will only focus on LQs coupled dominantly to third generation fermions (t, b, τ, ν_τ).

Fig. 2a shows the constraints on the coupling $\{\lambda = [x_1^L]_{33}$ in Eq. (1)$\}$ and mass of a vector LQ (such as the U_1), as derived from the different channels measured by the CMS collaboration [9].

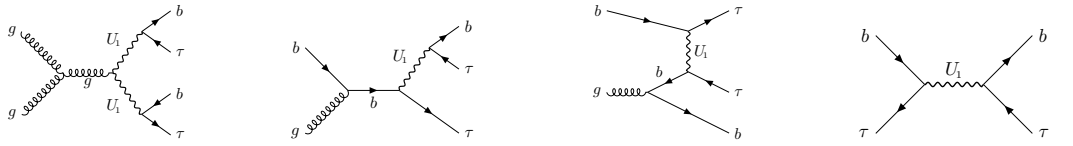

(a) Pair production. **(b)** Single production. **(c)** Drell-Yan. **(d)** Quark-lepton fusion.

Figure 1: Feynman diagrams contributing to LHC searches for the U_1 LQ (dominantly coupled to third generation fermions) in final states containing b jets and τ leptons.

Since pair production is QCD initiated, its constraint (red) does not depend on the LQ couplings and thus sets a lower bound for the LQ mass. Single production (green) is particularly sensitive to small masses, where the LQ can go on-shell. On the other hand, non-resonant Drell-Yan production (yellow) approximately constrains the coupling-over-mass ratio, and thus provides the dominating limits for high masses. Overall, an important complementarity of the different channels can be observed, yielding the combined limit (black). The resonant LQ production in quark-lepton fusion is not included here, and was only recently analyzed for scalar LQs in [10]. Similar to the single production it is mostly sensitive to the low mass region, where the LQ can go on-shell. While the quark-lepton fusion channel is not yet competitive, it might offer a unique possibility to probe resonant LQs signals in the future with higher statistics at the upcoming HL-LHC.

2.2 Third generation leptoquark production in association with b-tagged jets

A crucial feature of signals from LQs coupled to the third generation fermions are associated b-jets. As shown in Fig. 2 for the example of a U_1 LQ, these b-jets can be produced not only in the final state by the LQ decay, but also in the initial state through a gluon splitting in to a $b\bar{b}$ pair. Requiring associated b-jets can significantly reduce the background for LQ searches and thus improve the sensitivity [11]. This is further highlighted in Fig. 2b, where the constraints on the effective U_1 mass $\Lambda_U = M_U/[x_1^L]_{33}$ as a function of the relative strength of the coupling to right-handed fermions β_R is shown for an ATLAS [12] and a CMS [13] Drell-Yan search. For both cases, the constraints derived from the "b-tag" channel, where at least one b-jet is required in the final state, is more sensitive than the "b-veto" channel. Moreover, due to an inconclusive $\sim 3\sigma$ excess in the CMS search (gray), it is less sensitive than the ATLAS search, which is not optimized for LQ signals and where this excess is not observed. See also [14] for an optimized LQ search by ATLAS.

3. Leptoquark models in light of the B-meson anomalies $R_{D^{(*)}}$

As mentioned in Sec. 1, LQ models can offer a compelling explanation of the $R_{D^{(*)}}$ anomalies with the current experimental world averages $R_{D^{(*)}}^{\text{exp}}$ and the SM predictions $R_{D^{(*)}}^{\text{SM}}$ given by [3]

$$R_{D^{(*)}} = \frac{\mathcal{B}(B \to D^{(*)}\tau\nu)}{\mathcal{B}(B \to D^{(*)}\ell\nu)}\,, \text{ with } \ell \in \{\mu, e\}\,, \quad \begin{aligned} R_D^{\text{exp}} &= 0.342 \pm 0.026\,, \quad R_D^{\text{SM}} = 0.298 \pm 0.004\,, \\ R_{D^*}^{\text{exp}} &= 0.287 \pm 0.012\,, \quad R_{D^*}^{\text{SM}} = 0.254 \pm 0.005\,. \end{aligned} \tag{2}$$

As stated before, only the three LQ models commonly named U_1, S_1, and R_2, with their Lagrangians given in Eq. (1), are capable of addressing these anomalies [4]. We will discuss them in turn below based on [7], see also [4, 16].

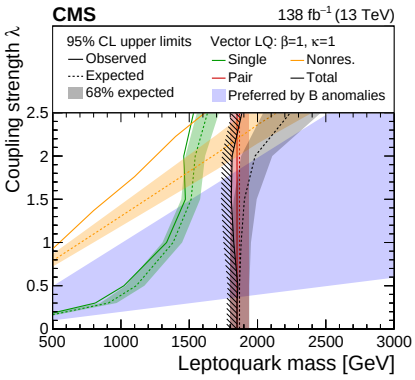

(a) Constraints from various LQ channels.

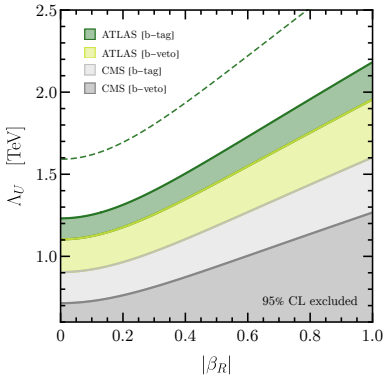

(b) Importance of tagging associated b-jets.

Figure 2: (a): Constraints from CMS searches for various LQ channels. Fig. taken from [9] (CC BY 4.0). (b): Comparison of different ATLAS and CMS Drell-Yan searches, and of channels with and without associated b-tagged jets in the final state. Shown are the constraints on the effective NP scale of the U_1 LQ Λ_U as a function of the coupling strength to right-handed fermions $\beta_R = \frac{[x_1^R]_{33}}{[x_1^L]_{33}}$. Fig. taken from [15].

3.1 Current status of the U_1, S_1, and R_2 leptoquark models in light of the B-anomalies

The current status of the $R_{D^{(*)}}$ explanation by the U_1, S_1, and R_2 models is summarized in Fig. 3, where the available range of couplings that are required for the explanation of the anomalies is shown for a reference LQ mass of 2 TeV. The preferred region by the B-anomalies is shown in blue, whereas electroweak constraints are given in gray. The limits from the Drell-Yan ATLAS searches [12, 17] for $pp \to \tau\tau/\tau\nu$ derived with the `HighPT` package [18] are shown in red, with the HL-LHC projections indicated by the dashed lines. The preferred region determined from a combined fit is shown in green. The different shadings refer to the 1σ and 2σ ranges in all cases.

The complementarity of the different data sets is visible for all three models considered. In particular, the Drell-Yan constraints break the flat directions of the flavor and the electroweak fits. For the U_1 and S_1 models we find a good agreement between the different data sets.[1] For the R_2 LQ, on the other hand, the different data sets are already in tension ($\lesssim 2\sigma$) and future HL-LHC data will be able to rule out this model.[2]

3.2 Future perspectives for the U_1 vector leptoquark

Also for the case of a U_1 LQ, future high-p_T Drell-Yan measurements will be able to rule out large parts of the parameter space. Fig. 4 shows in orange/purple the U_1 parameter region able to explain the measured $R_{D^{(*)}}$ values in the coupling-vs-mass plane $\left(g_U = \sqrt{2}[x_1^L]_{33}\right)$. On the left, only couplings to left-handed fermions are considered, whereas equal coupling strength for left- and right-handed fermions is assumed on the right. The plots are overlaid with the LHC constraints from LQ pair production and the Drell-Yan measurements from ATLAS [12] (green) and CMS [13] (gray). The scenario with only left-handed couplings is less constrained than the scenario with left- and right-handed couplings by current LHC data. As mentioned before, the

[1] For the S_1 LQ, $[y_1^L]_{33}$ couples the τ lepton to the top quark rather than the bottom and is thus only weakly constrained by LHC data, due to the suppressed top PDF.

[2] The R_2 LQ requires larger couplings to explain the B-anomalies, and is thus more constrained by LHC data.

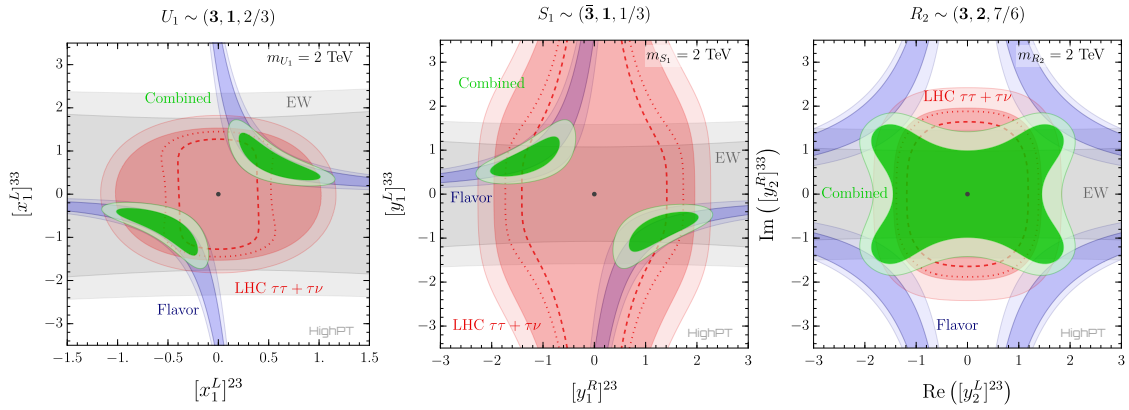

(a) U_1 vector LQ. **(b)** S_1 scalar LQ. **(c)** R_2 scalar LQ.

Figure 3: Constraints on the couplings of the U_1, S_1, and R_2 LQs that can address the charged-current B-anomalies. The 1σ and 2σ contours from "Flavor" ($R_{D^{(*)}}$), "LHC" (Drell-Yan), and "EW" (electroweak) limits are shown in blue, red, and gray respectively, whereas the "Combined" fit is given in green. The HL-LHC projections for 3 ab^{-1} are given by the dotted and dashed lines. Figure adapted and updated from [7].

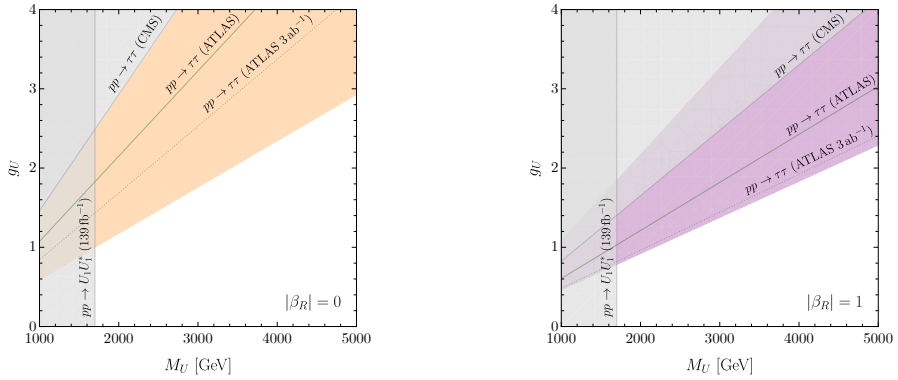

(a) **(b)**

Figure 4: (a): Coupling-vs-mass plot for the U_1 LQ coupled to left-handed fermions only. The region preferred by the $R_{D^{(*)}}$ measurements is given in orange and different LHC limits are shown. (b): Same plot as (a), but considering also couplings to right-handed fermions with equal strength. Fig. adapted from [15].

CMS limits are relaxed due to a $\sim 3\sigma$ excess in this search, which is not observed by ATLAS, see also [14]. Thus, if interpreted as a sign of NP, the CMS results would indicate a preference for right-handed couplings [15]. Furthermore, the dotted lines represent the HL-LHC projections which indicate that the U_1 scenario with right-handed couplings can be completely probed with future data, highlighting the importance of Drell-Yan data for scrutinizing the origin of the B-anomalies.

4. Conclusion

We have presented the current status of LQ searches at the LHC, discussed the different channels for these searches, and highlighted their complementarity. In addition, we discussed the improvement in sensitivity for third generation LQ models, when considering associated b-jets in the final state signatures. Thereafter, we focused on LQ models that can address the $R_{D^{(*)}}$ anomalies. In particular, we showed the crucial complementarity of low-energy flavor, electroweak, and high-

p_T Drell-Yan data in scrutinizing LQ models addressing these anomalies. Future data by LHC run-III and the HL-LHC will allow to further constrain these models and might help to unravel the origin of the B-anomalies. Not only future Drell-Yan data will be relevant for that, but with the increased statistics at HL-LHC, resonant LQ production in quark-lepton fusion will become a new and promising channel for discovery of LQ states.

Acknowledgments

I would like to thank the organizers of the *12th LHCP Conference* for the invitation and for supporting the participation with an *Early Career Researcher Grant*. I am very grateful to my colleagues J. Aebischer, L. Allwicher, D. Faroughy, G. Isidori, F. Jaffredo, M. Pesut, B. Stefanek, and O. Sumensari for their collaboration on different projects related to this presentation. FW has received funding from the Deutsche Forschungsgemeinschaft (DFG, German Research Foundation) under grant 396021762 – TRR 257: Particle Physics Phenomenology after the Higgs Discovery.

References

[1] W. Buchmuller, R. Ruckl and D. Wyler, *Phys. Lett. B* **191** (1987) 442.

[2] I. Doršner, S. Fajfer, A. Greljo, J.F. Kamenik and N. Košnik, *Phys. Rept.* **641** (2016) 1 [1603.04993].

[3] HFLAV collaboration, "Preliminary average of R_D and R_{D^*} for Moriond 2024." https://hflav.web.cern.ch/content/semileptonic-b-decays.

[4] A. Angelescu, D. Bečirević, D.A. Faroughy, F. Jaffredo and O. Sumensari, *Phys. Rev. D* **104** (2021) 055017 [2103.12504].

[5] L. Calibbi, A. Crivellin and T. Ota, *Phys. Rev. Lett.* **115** (2015) 181801 [1506.02661].

[6] C. Cornella, D.A. Faroughy, J. Fuentes-Martin, G. Isidori and M. Neubert, *JHEP* **08** (2021) 050 [2103.16558].

[7] L. Allwicher, D.A. Faroughy, F. Jaffredo, O. Sumensari and F. Wilsch, *JHEP* **03** (2023) 064 [2207.10714].

[8] L. Buonocore, P. Nason, F. Tramontano and G. Zanderighi, *JHEP* **08** (2020) 019 [2005.06477].

[9] CMS collaboration, *JHEP* **05** (2024) 311 [2308.07826].

[10] CMS collaboration, *Phys. Rev. Lett.* **132** (2024) 061801 [2308.06143].

[11] U. Haisch, L. Schnell and S. Schulte, *JHEP* **11** (2022) 106 [2207.00356].

[12] ATLAS collaboration, *Phys. Rev. Lett.* **125** (2020) 051801 [2002.12223].

[13] CMS collaboration, *JHEP* **07** (2023) 073 [2208.02717].

[14] ATLAS collaboration, *JHEP* **10** (2023) 001 [2305.15962].

[15] J. Aebischer, G. Isidori, M. Pesut, B.A. Stefanek and F. Wilsch, *Eur. Phys. J. C* **83** (2023) 153 [2210.13422].

[16] D. Bečirević, S. Fajfer, N. Košnik and L. Pavičić, *Phys. Rev. D* **110** (2024) 055023 [2404.16772].

[17] ATLAS collaboration, *Phys. Rev. D* **109** (2024) 112008 [2402.16576].

[18] L. Allwicher, D.A. Faroughy, F. Jaffredo, O. Sumensari and F. Wilsch, *Comput. Phys. Commun.* **289** (2023) 108749 [2207.10756].